Hyper–Rayleigh Scattering Studies of Model Imaging Materials

Amy Rassbach and M. R. V. Sahyun▲*

Department of Chemistry, University of Wisconsin—Eau Claire, Eau Claire, Wisconsin

We have shown by use of HRS spectroscopy that AgBr nanoparticles exhibit a first hyperpolarizability comparable to materials under consideration for optical technology applications. The technique enabled us to discover the unexpected quantitative conversion of AgBr into the Ag(**TAI**) complex on treating AgBr nanoparticles with **TAI**. This result suggests that **TAI** may function as a silver halide solvent under photographic conditions, with hitherto unconsidered consequences for grain architectural features of small radius. Results on dye adsorption demonstrate that HRS may be a powerful analytical tool for studying the adsorption of dyes on photographic silver halide grain surfaces. From the spectral dispersion of the HRS signals we can identify resonances with electronic transitions of the dyed and undyed particles. These transitions may also be important in their photophysics.

Journal of Imaging Science and Technology 45: 254–258 (2001)

Introduction

Hyper–Rayleigh Scattering Spectroscopy (HRS) is an incoherent spectroscopy for measurement of second harmonic generation by molecules in condensed phases.[1,2] The HRS signal may arise from a non-centrosymmetric chromophore or from an instant anisotropy that breaks the symmetry of the probe molecule and its solvation shell, i.e., symmetry reducing perturbations.[3] It is ideally suited to the study of molecules at interfaces, as well as colloidal particles,[3,4] where the signal may arise from solvent molecules oriented by the surface charge on the particle,[4] as well as from the chromophores in the particle itself, usually surface states. As an incoherent spectroscopy, HRS does not require a coherent excitation source and allows second harmonic signals to be observed with pump powers of the order of 0.05 – 5 watt.[5] Its signal is a measure of the molecular hyperpolarizability, β, which is commonly predicted by the two-level expression[5,6]

$$<\beta>= (3\ \mathbf{r}^2\Delta\mu)\{E_{op}^2/\left|2[E_{op}^2 - (h\omega)^2][E_{op}^2 - 4(h\omega)^2]\right|\} \quad (1)$$

where **r** is the transition dipole, evaluated from the absorption spectrum in the usual manner, Δμ is the change in dipole moment between ground (S_o) and first excited (S_1) states, E_{op} is the energy of the principal optical transition, and $h\omega$ is the photon energy of the probe radiation. Strictly speaking, Eq. 1 is applicable only insofar as the hyperpolarizability is associated with a charge–transfer electronic transition.[6]

In HRS the measured signal, the second harmonic intensity, $I(2\omega)$, may be expressed as

$$I(2\omega) = G(N_s\beta_s^2 + N_a\beta_a^2)[I(\omega)]^2 \quad (2)$$

where G is a proportionality constant, reflecting signal collection efficiency, etc., N designates the number density of the solvent (subscript s) or solute (subscript a)[1,2] molecules. The observable product, $G\beta_a^2$, is usually called the quadratic coefficient. In practice the first term of Eq. 2 also includes contributions from adventitious scattered second harmonic radiation, which makes evaluation of the quadratic coefficient of the solvent, e.g., as internal standard, problematical. Therefore in practice, Eq. 2 we rearrange

$$I_{obs} = (I(2\omega)/I(\omega) - GI(\omega)N_s\beta_s^2) = GI(\omega)N_a\beta_a^2 \quad (3)$$

where $I_{obs} = [I(2\omega)/I(\omega)]$, and we refer to the measured slope of the I_{obs} versus N_a regression analysis as the relative quadratic coefficient.

Given the importance of interfacial phenomena to photoimaging processes, especially silver halide photography, we have undertaken a program to establish the utility of HRS to the study of imaging materials and processes. In this article we report the first results of this endeavor.

Experimental

Materials

Dye **I**, 5–[(3–ethyl–2(3H)–benzoxazolylidene) ethylidene]–4–oxo–2–thioxo–3–thiazolidineacetic acid, was used as received from H. W. Sands Co., Jupiter, FL; in methanol solution it exhibits[7] λ_{max} = 492 nm with molar extinction coefficient $3.3 \times 10^4\ M^{-1}cm^{-1}$. The absorption red shifts to ca. 508 nm on adsorption of the dye to AgBr. A molecular mechanics optimized (Merck Molecular Force Field) structure of the dye is shown in Fig. 1. The 4–hydroxy–6–methyl–1,3,3a,7–tetraazaindene (**TAI**), m– and p–nitroaniline (**MNA** and **PNA**) were all of 99+ % purity and likewise used as received from Aldrich Chemical Co., Milwaukee, WI. Spectrograde methanol (Spectra Products, Gardena, CA) was used for preparation of solutions.

Original manuscript received August 28, 2000

▲ IS&T Member

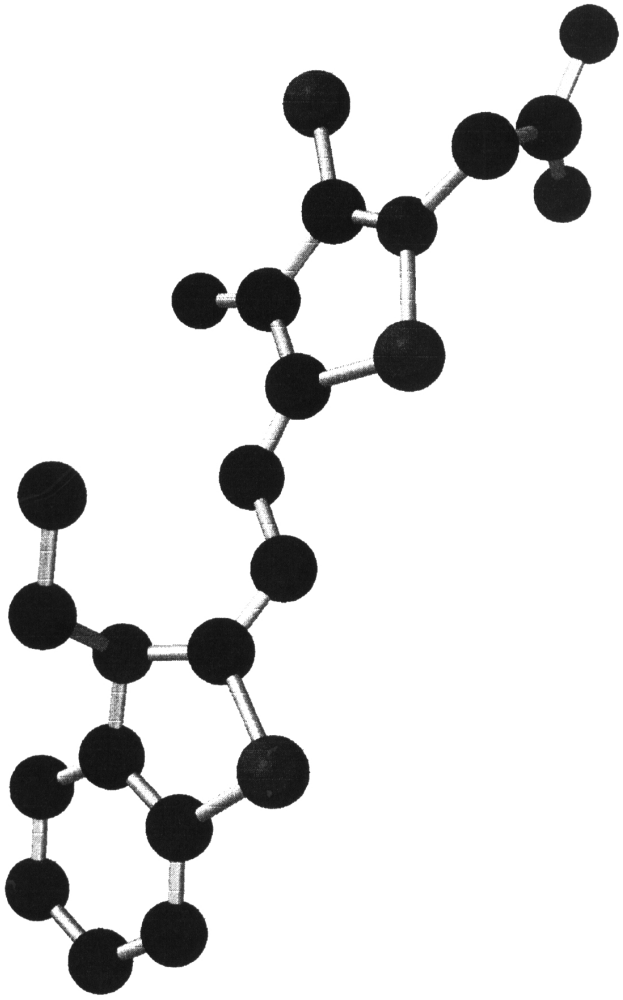

Figure 1. Molecular mechanics optimized structure of Dye **I**.

Silver halide nanoparticles were prepared in methanol in the manner previously described[8–10] from tetrabutylammonium bromide and silver tetra-fluoroborate, using a high hydroxyl content polyvinylbutyral (BX-L from Sekisui Chemical Co., Japan) as protective colloid. In our hands this method produced very stable dispersions of particles, previously characterized[9] as 6–10 nm in diameter. These estimates have been confirmed on various preparations of the colloid by x-ray diffraction, absorption band edge measurements, and dye adsorption. Fresh preparations were used for each experiment.

Methods

The optical set-up for detection of HRS is shown in Fig. 2. Light from a 150 watt Xe arc lamp is passed through a grating monochromator, set to 900 nm with a 2 nm bandpass, and a chopper. The pump beam impinges on a solution sample in a 1 cm quartz cuvette. Scattered radiation is detected at right angles to the pump beam by a Hamamatsu model 933 photomultiplier with lock-in amplification, through a second monochromator tuned to the second harmonic wavelength, 450 nm. The signal is ratioed to that of a matched photomultiplier monitoring the pump beam; hence the measured signal corresponds to $I(2\omega)/I(\omega)$, i.e., I_{obs} in Eq. 3. A polarizing filter in the detector path was employed to minimize contribution to the signal from second harmonic generated by scattering off the optical surfaces and second harmonic of the fundamental adventitiously passed by the monochromator. Optical components were derived from the optical table of a Perkin–Elmer model MPF-44B spectrofluorimeter.

As a standard procedure, detection of HRS was undertaken as follows. A 2.5 mL portion of the solvent (spectrograde methanol or toluene, Aldrich Chemical Co.) was placed in the sample cuvette, and the signal detector was set to zero. Aliquots (usually 25 μL) of a probe solution were then added, and the signal recorded

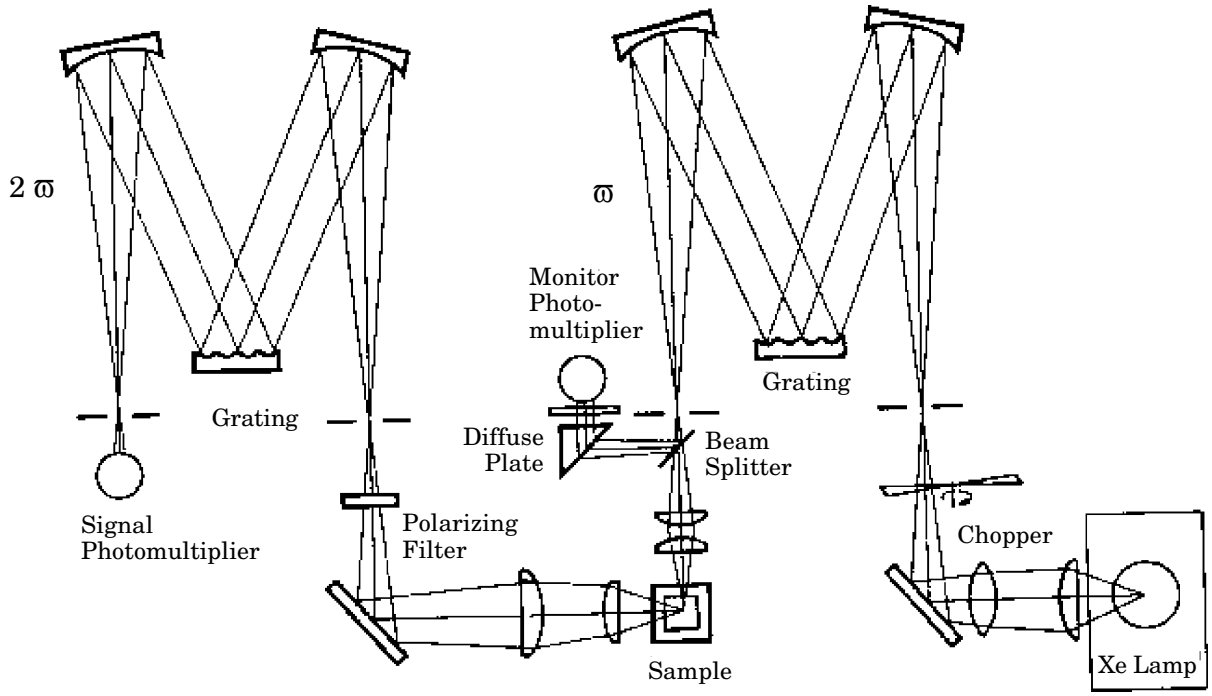

Figure 2. Optical scheme for the detection of hyper-Rayleigh scattering (HRS).

after each. A minimum of three replications of each experiment was required to provide data suitable for analysis, along with estimates of confidence limits for the values obtained thereby. Eq. 3 was used for data analysis; the detector circuit was nulled so as to obtain $I_{obs} = 0$ for $N_a = 0$. Values of the relative quadratic coefficient were then determined by least-squares fitting of the experimental data.

Spectral dispersion of HRS was measured by variation of ω, while monitoring response of the 2ω signal. Observed signals were corrected for spectral variation in instrument sensitivity, and normalized to values obtained for 2ω = 450 nm. Significant fall-off in instrument response was not observed until 2ω ≤ 340 nm.

Two criteria were met to confirm that the observed signals were, indeed, HRS: (1) except as noted below, the amplitude of the observed signal was directly proportional to the concentration of added solute as predicted by Eq. 3, i.e., the quadratic coefficient was independent of solute concentration; and (2) the output radiation was monochromatic, distributed over a bandpass comparable to the fundamental beam slit width.

Results and Discussion

In the context of ongoing studies of the relaxation pathways in cyanine chromophores, we had undertaken[11] studies of three prototypical spectral sensitizing dyes, N,N'-diethyl-2,2'-dithiacyanine iodide (**DCI**), N,N'-diethyl-2,2'-carbocyanine iodide (**DTCI**), and N,N'-diethyl-2,2'-dicarbocyanine iodide (**DTDCI**), all of which yielded large HRS signals in methanol indicative of large first hyperpolarizabilities, β. These were estimated by comparison to the relative quadratic coefficients of *m*– and *p*–nitroaniline (**MNA** and **PNA**, respectively)[5] measured under the same conditions. Interestingly, the HRS response of the analogous tricarbocyanine iodide (**DTTCI**) was not detectable under our conditions. The HRS signal from **DTCI** disappeared completely when the experiment was carried out in toluene. On this basis we inferred that the first hyperpolarizability was a property of the chromophore-solvation shell ensemble, and not of the dye cation by itself. In this connection the role of oriented solvent molecules in producing second harmonic response from the surface of colloidal molecules[4] is of significance.

Non-linear Optical Properties of AgBr. We have previously demonstrated the optical limiting characteristics of nanoparticulate AgBr[10]; use of HRS allowed us to explore another non-linear response, namely hyperpolarizability. Addition of aliquots of 1×10^{-4} M silver bromide nanosol to the sample cuvette led to the HRS signals shown in Fig. 3. From the least squares analysis, the relative quadratic coefficient is $(9.6 \pm 1.6) \times 10^6$ M^{-1}. By comparison to the relative quadratic coefficient obtained for **PNA** under comparable conditions, for which the accepted value[5] of $\beta = 30 \times 10^{-30}$ esu, we estimate for nanoparticulate AgBr, β = ca. 100×10^{-30} esu, of sufficient magnitude to be of interest for device, e.g., optical communications, applications. The value is not as large as observed for nanometals,[3] but comparable to that observed for other colloidal insulators, e.g., SiO_2.[12] On a per particle basis (assuming 6 nm particle diameter; see below), a first hyperpolarizability of ca. 2.5×10^{-25} esu may be estimated, substantially greater than found for comparably sized CdSe particles.[13]

The corrected wavelength dispersion of the HRS signal from the AgBr nanosol is shown in Fig. 4. From Eq. 1 we expect a maximum in the hyperpolarizability to be observed when either ω or 2ω corresponds to an allowed electronic transition, which may be coupled by the second harmonic generation process. In Fig. 4 we observe such a maximum at ca. 355 nm, (3.50 ± .05) eV. We assign this transition to a surface state of the AgBr nanoparticles. Band structure calculations[14] on the reorganized AgBr (111) surface indicate that direct transitions are possible at the surface between bromide-

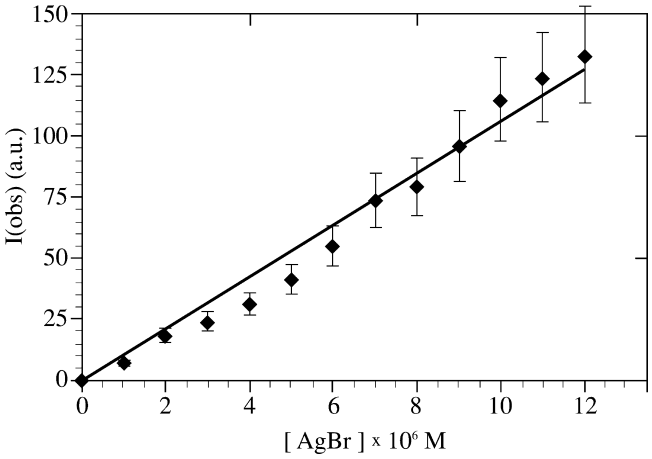

Figure 3. Concentration dependence of HRS signal from AgBr nanosol; N_s is "molecular" concentration of AgBr.

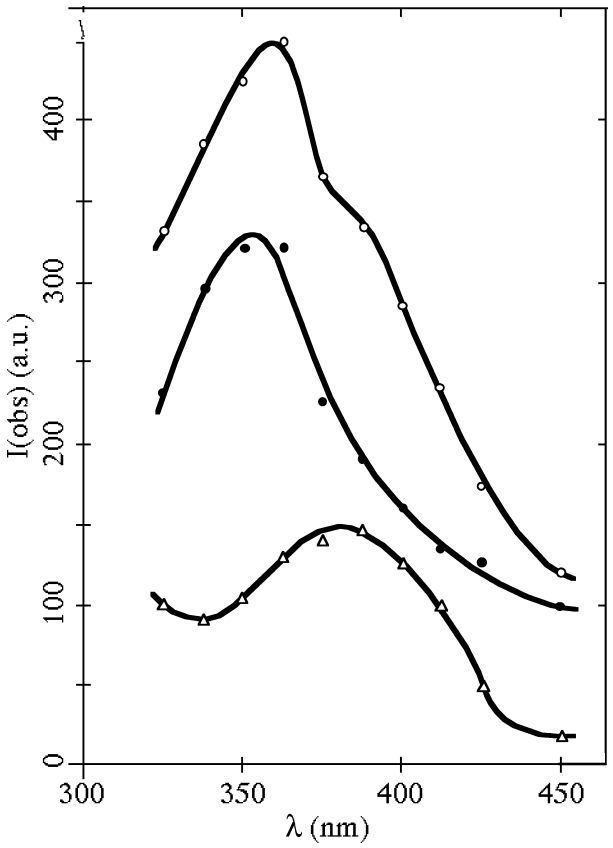

Figure 4. Spectral dispersion of HRS response with 2ω wavelength for AgBr nanosol (solid circles), dyed AgBr (open circles), and chemisorbed Dye **I** (triangles). Solid lines are only to guide the eye.

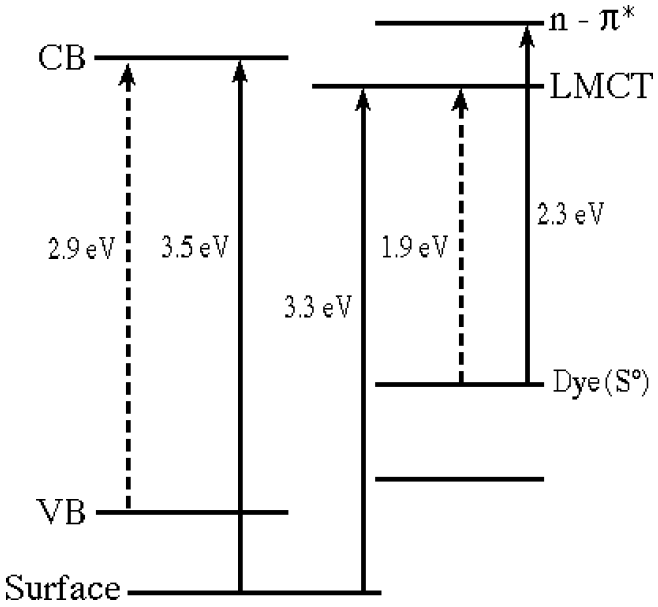

Figure 5. Scheme of hypothetical electronic transitions that couple with the second harmonic generation process.

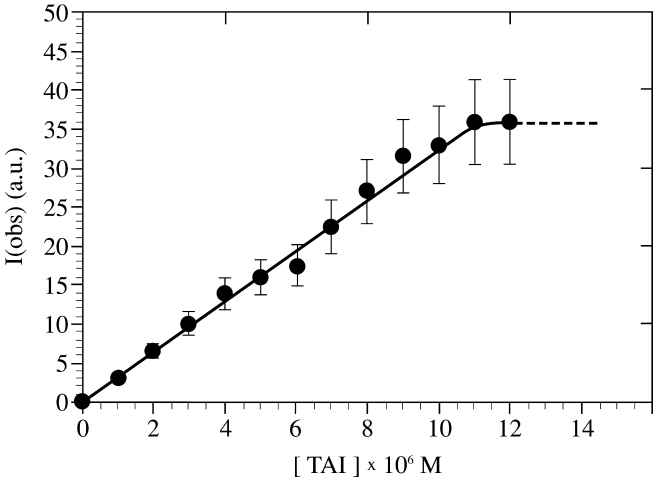

Figure 6. Reaction of nanoparticulate AgBr with **TAI**, monitored by HRS. N_s is molecular concentration of **TAI**, where [AgBr] = 1×10^{-5} M.

centered levels within the valence band and localized Ag–*s* levels at or near the bottom of the conduction band. Note that the inferred transition energy is ultra-band gap for these particles, wherein E_g = 2.9 eV.[9] A hypothetical energy level diagram for states of the AgBr nanoparticles, which may be coupled to second harmonic generation, is presented as Fig. 5.

***Reaction with* TAI.** Because the HRS signals observed from the nanosol most likely arise from surface states of the AgBr particles, we next sought to ascertain the consequences of deliberate surface modification of the particles. To this end we chose 4-hydroxy-6-methyl-1,3,3a,7-tetraazaindene (**TAI**) as the surface reagent. Its adsorption to AgBr by reaction of the **TAI** anion with interstitial silver ions is well-documented.[15] To simplify the experiment by eliminating the complication of the ionization equilibrium (pK_a = 6.53)[16] of **TAI**, we monitored HRS on addition of 25 μL aliquots of 10^{-4} M **TAI** in 0.001 NaOH (methanol) to 1×10^{-5} M AgBr nanosol. Results are shown in Fig. 6. In this case, I_{obs} increases linearly with [**TAI**] as expected on the basis of Eq. 3 until the eleventh aliquot, where [**TAI**] = 1×10^{-5} M, i.e., exactly equivalent to [AgBr]. Subsequently, no further growth in I_{obs} occurs. No HRS signal is obtained from the **TAI** solution in absence of AgBr.

We interpret these results in terms of a stoichiometric, heterogeneous reaction between **TAI** and AgBr

$$\mathbf{TAI}^- + \mathrm{AgBr} \rightarrow \mathrm{Ag}(\mathbf{TAI}) + \mathrm{Br}^- \qquad (4)$$

which is driven to completion by the excess surface free energy of the nanoparticles. The quadratic coefficient obtained from the least squares analysis of Fig. 6 is (3.3 ± .2) × 10^{-6} M. However, according to the chemistry of Eq. 4, the observed signal comprises

$$I_{obs} = GI(\omega)[\beta^2(\mathbf{TAI}) - \beta^2(\mathrm{AgBr})]N_a \qquad (5)$$

Accordingly we estimate β = 70 × 10^{-30} esu for the Ag(**TAI**) complex, again by comparison to **PNA** as standard. The large hyperpolarizability of this complex is probably associated with a ligand-to-metal charge transfer transition.

One implication of Eq. 4 is that **TAI** may have significant silver halide solvent activity, even under photographic conditions, especially with respect to grain features of small radius of curvature, e.g., corners, defects, and epitaxial growths. This possibility seems to have been overlooked in previous discussions of the photographic effects of **TAI**. In water, the solubility product of Ag(**TAI**) is low (K_{sp} = 10.8)[16] but significant.

Sensitizing Dye Adsorption. Adsorption of dyes to silver halide surfaces is a critical element of photographic technology. It was of interest to us to see if we could demonstrate the utility of HRS as an analytical tool for following the adsorption of dye to AgBr. In order to unequivocally assign HRS signals to adsorbed dye, vis-à-vis free dye in solution, it was necessary to employ a sensitizing dye that did not yield significant HRS response in solution. In addition, dyes such as **DTCI** would be inappropriate for this demonstration, as they would introduce the iodide counterion into the system which might, in turn, also give rise to HRS signals on interaction with the nanoparticle surface. Dye **I** was found to satisfy the first requirement, without introducing a reactive counterion which might change the surface chemistry of the nanoparticle. Its benzthiazolylidene analog was previously used in our laboratory to study spectral sensitization of photolysis[9] and optical limiting[10] of nanoparticulate AgBr. Both dyes are expected to chemisorb to AgBr through formation of a chelate of surface silver ion, involving the thiazolidine-N-acetic acid moiety of the dye[17], i.e., a chemisorptive mechanism of dye interaction with AgBr is expected.

Strong HRS signals were obtained when aliquots of a 10^{-5} M solution of dye **I** in methanol were added to 1×10^{-5} M AgBr nanosol. However, Eq. 3 did not apply, as shown in Fig. 7a. The experimental results could be linearized by application of the Langmuir adsorption isotherm:

$$(1/I_{obs}) = (1/I_\infty)(1 + 1/K[\mathrm{Dye}]) \qquad (6)$$

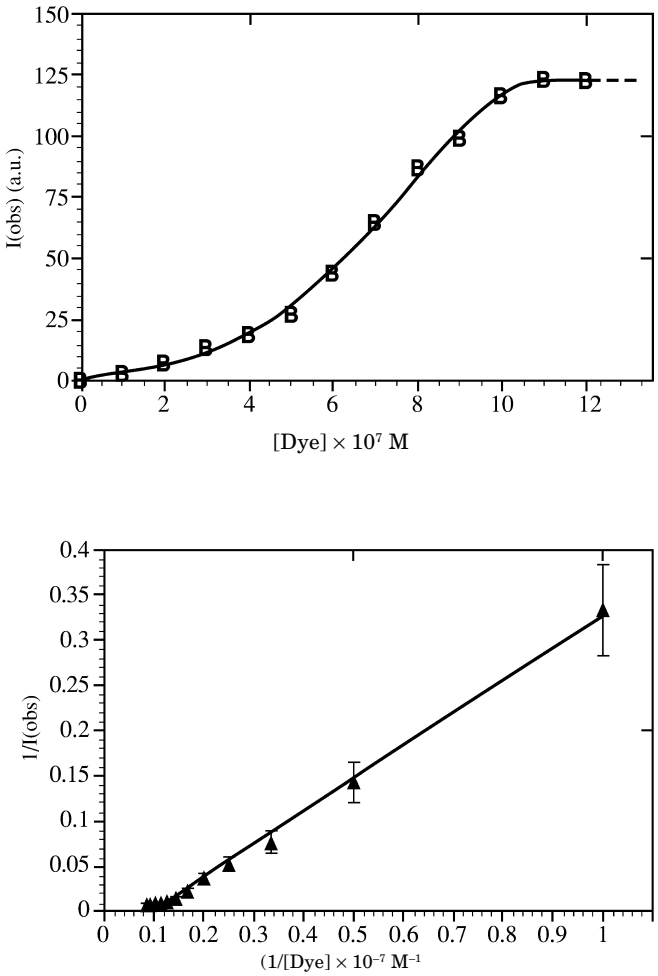

Figure 7. Adsorption of Dye **I** to nanoparticulate AgBr monitored by HRS: (a) data as recorded; (b) data as interpreted according to the Langmuir adsorption isotherm.

where K is the equilibrium coefficient for adsorption, and I_∞ is the value of I_{obs} at saturation. The fit to Eq. 6 is shown in Fig. 7(b), where saturation occurs after the eleventh aliquot, where [Dye] ≥ ca. 1×10^{-6} M, and K = 2.2×10^5 M^{-1}, with r = 0.999. Note that when the benzthiazolylidene analog of dye **I** was used[9,10] and adsorption monitored by absorption and fluorescence spectroscopies, it was necessary to use a Freundlich isotherm to describe dye adsorption. That result suggested a distribution of adsorption sites on the nanoparticle surface, while the present results suggest a more-or-less homogeneous surface for dye adsorption.[18] The large value of K is consistent with chemisorption.

The fit allows estimation of a relative quadratic coefficient of 1.3×10^8 M^{-1} for the dye adsorbate, corresponding to a very large $\beta = 3.6 \times 10^{-28}$ esu, within an order of magnitude of the upper limit observed for molecular systems.[19] We hypothesize that the dye concentration where the HRS signal saturates, i.e., reaches I_∞, corresponds to monolayer coverage of spherical AgBr particles. Accordingly we estimate an average particle size of 6 nm in diameter, given a projection area of 50 Å^2 for individual adsorbed dye molecules based on the molecular mechanics calculation, above, and an assumption of edge-on adsorption, as assumed previously.[9] We take this result as a confirmation of the expected particle size of the AgBr nanocrystals.

The spectral dispersion of the HRS signal for the AgBr nanosol with a monolayer of adsorbed dye is also shown in Fig. 4. Because the observed signals in this case are composites of $[I(2\omega)/I(\omega)]$ for both AgBr and adsorbed dye, the signals measured for AgBr alone were subtracted from the composite signal, to obtain the dispersion curve for adsorbed dye, alone, also shown in Fig. 4. Its maximum occurs at ca. 385 nm, i.e., (3.29 ± .05) eV. One possible assignment for the corresponding electronic transition is between a surface state of AgBr and the LMCT state of the dye-silver ion complex, which was implicated in spectral sensitization with the benzthiazolylidene analog of dye **I**[9]. This assignment is reflected in the hypothetical scheme of Fig. 5. Previously,[10] however, we noted a maximum at 392 nm (3.25 eV) in the excitation spectrum for photoluminescence from undyed nanosol preparations, and assigned it to an iodide cluster centered transition.

Conclusions

We have shown by use of HRS spectroscopy that AgBr nanoparticles exhibit a first hyperpolarizability comparable to materials under consideration for optical technology applications. From the spectral dispersion of the HRS signal we can infer resonances with electronic transitions of the particles, which may also be important in their photophysics, e.g., surface states. The HRS technique also enabled us to discover the unexpected quantitative conversion of AgBr into the Ag(**TAI**) complex on treating AgBr nanoparticles with **TAI**. This result suggests that **TAI** may function as a silver halide solvent under photographic conditions, with hitherto unconsidered consequences for grain architectural features of small radius. Results on dye adsorption demonstrate that HRS may be a powerful analytical tool for studying the adsorption of dyes on photographic silver halide grain surfaces.

References

1. T. Verbiest, K. Clays, C. Samyn, J. Wolff, D. Reinhoudt, and A. Persoons, *J. Amer. Chem. Soc.* **116,** 9320 (1994).
2. K. Clays and A. Persoons, *Phys. Rev. Lett.* **66,** 2980 (1991).
3. F. W. Vance, B. I. Lemon and J. T. Hupp, *J. Phys. Chem. B* **102,** 10091 (1998).
4. E. C. Y. Yan and K. B. Eisenthal, *J. Phys. Chem. B*, **104,** 6686 (2000).
5. J. L. Oudar and D. S. Chemla, *J. Chem. Phys.* **66,** 2664 (1977).
6. D. Pugh and J. O. Morley, in *Nonlinear Properties of Organic Molecules and Crystals*, vol. 1, D. S. Chemla and J. Zyss, Eds., Academic Press, Orlando, FL, 1987, p. 206.
7. http://www.hwsands.com.
8. K.P. Johansson, G. McLendon and A. P. Marchetti, *Chem. Phys. Lett.* **179,** 321 (1991).
9. M. R. V. Sahyun, D. K. Sharma and N. Serpone, *J. Imaging Sci. Technol.* **39,** 377 (1995).
10. M. R. V. Sahyun, S. E. Hill, N. Serpone, R. Danesh, and D. K. Sharma, *J. Appl. Phys.* **79,** 8030 (1996).
11. A. F. Marks, A. K. Noah and M. R. V. Sahyun, *J. Photochem. Photobiol. A: Chem.* **139,** 143 (2001).
12. F. W. Vance, B. I. Lemon, J. A. Ekhoff, and J. T. Hupp, *J. Phys. Chem. B* **102,** 1845 (1998).
13. M. Jacobsohn and U. Banin, *J. Phys. Chem. B* **104,** 1 (2000).
14. A.-S.Malik, F. J. DiSalvo, R. Hoffmann, and J. T. Blair, *J. Imaging Sci. Technol.* **42,** 210 (1998).
15. (a) D.L. Smith and H. R. Luss, *Photogr. Sci. Eng.* **20,** 184 (1976); (b) T. Tani and M. Saito, *ibid.* **23,** 323 (1979); (c) D. D. F. Shiao, M. T. Nieh and A. H. Herz, *ibid.* **30,** 208 (1982).
16. T. Tani, *Photographic Sensitivity*, Oxford Univ. Press, Oxford, UK, 1995, p. 184.
17. T. A. Smith, J. G. DeWitt, B. Hedman, and K. O. Hodgson, *J. Amer. Chem. Soc.,* **116,** 3836 (1994).
18. A. W. Adamson, *Physical Chemistry of Surfaces*, 2nd ed., Interscience, New York, 1967, p. 400.
19. S. R. Marder, L. T. Cheng, B. G. Tiemann, A. C. Friedli, M. Blanchard-Desce, J. W. Perry, and J. Skinhøj, *Science* **263,** 511 (1994).